Alpha oscillations shape sensory representation and perceptual accuracy

Ying Joey Zhou[1], Luca Iemi[2], Jan-Mathijs Schoffelen[1], Floris P. de Lange[1], Saskia Haegens[1,2,3]

[1] Donders Institute for Brain, Cognition, and Behaviour, Radboud University

[2] Department of Psychiatry, Columbia University College of Physicians and Surgeons

[3] Division of Systems Neuroscience, New York State Psychiatric Institute

Corresponding author: Saskia Haegens (shaegens@gmail.com)

Author Contributions: YJZ, LI, FPdL, and SH designed the research; YJZ performed the research; YJZ, JMS, and SH analyzed the data; YJZ, LI, FPdL, and SH wrote the paper.

Competing Interest Statement: None.

Keywords: alpha oscillations; visual detection; signal detection theory

This PDF file includes:

Main Text
Figures 1 to 5

Abstract

Alpha oscillatory activity (8–14 Hz) is the dominant rhythm in the awake brain, and is thought to play an important role in setting the brain's internal state. Previous work has associated states of decreased alpha-band oscillatory power with enhanced neural excitability. However, opinions differ on whether and how such excitability enhancement modulates sensory signals of interest versus noise differently, and what, if any, the consequences are for the subsequent perceptual process. To address these questions, we used a novel paradigm to experimentally manipulate human subjects' decision criteria in a visual detection task. In different blocks, we primed subjects with clearly visible stimuli to introduce either a liberal or conservative detection criterion for subsequent ambiguous stimuli. While we observed substantial criterion shifts under different priming conditions, such criterion shifts were not reflected in pre-stimulus alpha-band changes. Rather, we found that lower pre-stimulus alpha-band power in early visual cortices improved perceptual accuracy, accompanied by enhanced information content decodable from the neural activity patterns. Additionally, we showed that alpha oscillatory phase in parietal and frontal regions immediately before stimulus presentation modulated accuracy. Together, our results suggest that alpha-band dynamics modulate sensory signals of interest more strongly compared to noise, here resulting in enhanced information coding and improved perceptual accuracy.

Significance Statement

The internal state of our brain fluctuates, giving rise to variability in perception and action. Neural oscillations, most prominently in the alpha-band, have been suggested to play a role in setting this internal state. Here, we show that ongoing alpha-band activity in early visual regions predicts the quality of visual information decodable in neural activity patterns, and subsequently human observer's accuracy in a visual detection task. Our results provide the heretofore first evidence that visual representation is modulated by ongoing alpha-band activity, and advance our understanding on how, when faced with unchanging external stimuli, internal neural fluctuations influence perception and behavior.

Introduction

The state we are in affects our performance. Think about the case of driving: a driver is more likely to catch a sign that appears briefly in her periphery when driving with full concentration, compared to when driving in a drowsy state. In experimental settings, when presented with the same threshold-level stimulus repeatedly, an observer will detect the stimulus in one instance but miss it in another. Understanding how otherwise identical stimuli lead to variable percepts has been a key challenge in neuroscience. One source of this perceptual variability is the brain's internal state, which is largely determined by moment-to-moment neural activity fluctuations (for reviews, see (1, 2)).

The alpha rhythm has been known as the dominant rhythm in the awake brain since its first discovery by Hans Berger (3). One prevailing hypothesis is that the alpha rhythm sets the internal state's level of excitability via a mechanism of functional inhibition (4, 5): for a population of neurons, its activity is inhibited when ongoing alpha oscillatory power is strong, and the extent of inhibition is temporally dependent on the alpha oscillatory phase. In support of this hypothesis, it has been demonstrated that alpha oscillatory amplitude correlates negatively with neural excitability (for review, see (1, 6)) as measured by spike firing rate (7), gamma-band power (8), BOLD activity amplitude (9), and the probability of perceiving TMS-induced phosphenes (10), and that the extent of this excitability modulation changes periodically as a function of oscillatory alpha phase (7, 11–13).

Because of its tight link with internal excitability, alpha-band oscillatory activity (and its temporal fluctuations) is a plausible key source of perceptual variability. Indeed, an extensive body of work has shown that pre-stimulus oscillatory alpha-band power modulates perception of both visual and somatosensory stimuli (14–18). Interestingly, only recently researchers have started to investigate *how* internal excitability changes indexed by alpha oscillations manifest in subjects' behavioral outcomes (19, 20), using the framework of Signal Detection Theory (21). In this framework, two metrics are used to quantify the perceptual process: discriminability (d') – a metric of how well the observer distinguishes sensory signals of interest from noise, and criterion (c) – a metric of observer's tendency for one perceptual decision over the others. Depending on potentially differential impacts on sensory signals of interest versus noise, internal excitability changes indexed by alpha activity may modulate different aspects of the perceptual process.

On the one hand, it is suggested that decreased alpha activity amplifies sensory signal of interest and noise to the same extent (e.g., the gain is *additive* to the response amplitude) without making them more distinct from each other, and therefore only results in a criterion shift in the observer's behavior (Figure 1). This view is mainly supported by empirical work correlating ongoing, as opposed to experimentally-induced, alpha activity changes with perceptual decisions. For example, several studies showed that when pre-stimulus alpha activity was low, subjects reported higher subjective visibility (22) and confidence (20), and had a higher tendency to see a target (i.e., more liberal criterion), but displayed no change in perceptual discriminability (19, 23). If a low state of alpha oscillations indeed amplifies signal and noise similarly and thereby shifts the observer's criterion, a key question is whether (top-down) changes in criterion are implemented via (and/or reflected by) shifts in the alpha state.

On the other hand, it is suggested that decreased alpha activity amplifies the signal of interest to a larger extent relative to the noise (e.g., the gain scales *multiplicatively* as a function of response amplitude), making them more distinct from each other and hence resulting in improved perceptual discriminability (Figure 1). This view is largely inferred based on studies using classical attentional-cueing paradigms, in which pre-stimulus alpha-band activity patterns (i.e., alpha lateralization, activity difference between task-relevant and task-irrelevant regions) and perceptual discriminability co-vary following attentional cueing (14–16). Although informative, it is unclear whether the observed correlation between pre-stimulus alpha lateralization and behavioral performance is mainly driven by an alpha amplitude decrease in task-relevant or increase in task-irrelevant regions. Furthermore, if alpha oscillations indeed modulate sensory signal of interest more strongly relative to the noise, an immediate prediction is that information coding of the task-relevant stimuli be enhanced in a state of low alpha activity.

To differentiate between these hypotheses, we tested human subjects in a magnetoencephalography (MEG) experiment, during which we experimentally manipulated their decision criterion using a novel visual detection paradigm. We examined whether and how changes in pre-stimulus alpha dynamics (*i*) correlate with criterion shifts in the detection task, (*ii*) influence perceptual discriminability while decision criterion is controlled, and (*iii*) modulate information coding, indexed by the representational content decodable in the neural signal.

Results

Priming leads to criterion shifts

Subjects finished eight blocks of the main experimental task and three blocks of a localizer task during the MEG session. For the localizer task, they had to detect and report as fast as possible occasional fixation changes, which occurred in 15% of all trials. Subjects correctly reported fixation changes on 99.5% (between-subjects SD = 0.5 %) of all trials with mean median reaction time (RT) of 406 ms (between-subjects SD = 49 ms), confirming close engagement in the task.

For the main experimental blocks, subject's task was to report the presence (or absence) of an oriented grating as accurately as possible. They consistently performed at ceiling during the priming phase when the masking effect was minimal (mean accuracy = 95.2%, with a between-subjects SD of 5.1%; mean median RT = 421 ms, with a between-subjects SD of 73 ms). For the main task trials, in which the mask was presented at a contrast level titrated for each subject, overall accuracy dropped to around 75% as aimed for. Note the mean accuracy was lower than that expected from a 3-down-1-up staircase procedure (i.e., about 80%), likely because the instructed target presence rate was different from the actual target presence rate. Two-way (priming type × grating orientation) repeated-measures ANOVA showed no significant differences across conditions in RT or accuracy (Fs < 1; Figure 2B). Results of the SDT analysis (Figure 2C) showed that subjects were significantly more liberal in reporting "target present" in the liberal priming blocks than in the conservative priming blocks (Wilcoxon sign-rank test, $p < 10^{-4}$), validating our experimental manipulation. Moreover, subjects exhibited a significantly higher discriminability (*d'*) in the conservative blocks (Wilcoxon sign-rank test, $p = 0.003$) than in the liberal blocks. The higher *d'* for conservative trials may be due to the more skewed mapping between the false alarm (FA) rate to its Z-value in our *d'* computation. Specifically, when criterion (or the decision boundary) intersects the noise distribution at its right tail, small changes in FA rate are nonlinearly exaggerated after Z-transformation. As we did not observe a difference in accuracy between conservative and liberal trials, which is a more robust measure of perceptual discriminability when target presence rate equals 50%, we argue that the observed statistically significant *d'* difference is equivocal. Further analysis showed that both hit and FA rates remained stable both within and across blocks, suggesting a sustained priming effect both within the block and between different blocks across the session (SI Results). Taken together, our behavioral results show that the current paradigm successfully introduces criterion shifts in subject's detection responses.

Priming does not lead to modulation of pre-stimulus oscillatory power or stimulus-evoked activity

According to the additive hypothesis, pre-stimulus alpha power modulates the decision criterion. Therefore, one may expect (top-down) changes in criterion induced by different priming conditions to be reflected in alpha power differences. We first compared pre-stimulus time-frequency representations (TFRs) between the conservative vs. liberal trials, without making any assumptions about the frequency range of potential effects. We observed no significant differences in pre-stimulus TFRs ($p = 0.366$, cluster-based permutation test with frequencies from 1 to 30 Hz, time points from 800 ms pre-stimulus to stimulus onset, including all sensors) between the two priming conditions. We then repeated our statistical tests by constraining our frequencies of interest to the alpha range (6 – 14 Hz), or by constraining the channels of interest to 20 subject-specific channels with strongest evoked response to the localizer gratings (in a time

window of [0.1, 0.2], relative to baseline). We found no significant pre-stimulus TFR differences between the two priming conditions in either analysis.

In addition to pre-stimulus activity, we examined whether priming modulates the sensory response amplitude to the stimuli. We constrained these analyses to the above-mentioned 20 subject-specific channels, which primarily reflect the stimulus-evoked responses. We did not observe any significant differences in the average event-related fields (ERF) amplitude (averaged across all selected sensors within each subject) between different priming conditions for the main task trials (SI Figure S2A). Interestingly, when the same contrasts were repeated for the priming trials, we found that for target-present trials, conservative priming led to larger ERF amplitude 400 to 650 ms after stimulus onset ($p < 10^{-4}$; Figure S2B solid lines) compared to liberal priming; and this pattern was reversed for target-absent trials ($p < 10^{-4}$; Figure S2B dotted lines). These observations may reflect a general P3 surprise effect (24) to the less frequently presented stimuli, given that target-present and target-absent trials were rare events (i.e., 20% of trials) in the conservative and liberal priming blocks respectively. These ERF results also suggest that subjects incorporated the different probabilistic information in sensory processing during the priming phase.

Taken together, we showed for the main task trials that neither the pre-stimulus oscillatory activity nor the stimulus-evoked activity reflects the (top-down) criterion changes introduced by priming.

Pre-stimulus alpha power modulates *d'*: region of interest analysis

If excitability modulation by alpha oscillatory power has any behavioral consequence, its magnitude immediately prior to stimulus onset, within the neuronal populations most responsive to the stimuli, should be most relevant for subsequent detection responses. Following this rationale, we zoomed in to the anatomical parcel most responsive to localizer gratings (defined for each subject, see Figure 3 for spatial topography of the selected parcels), and asked whether and how alpha power immediately before the stimulus onset in these functionally defined visual regions of interest (ROIs) predict subject's responses.

We first examined whether pre-stimulus oscillatory activity in these ROIs differed between the conservatively and liberally primed trials. While we observed prominent oscillatory activity within the alpha-band during the pre-stimulus time window (Figure 3C), we found no significant difference between the two conditions in both the pre-stimulus TFR (cluster-based permutation test with frequencies from 1 to 30 Hz, time points from 800 ms pre-stimulus to stimulus onset: $p = 0.257$) and power spectrum (cluster-based permutation test with all frequencies: $p = 0.078$).

To capture more subtle effects of pre-stimulus oscillatory alpha power on detection responses, we then grouped trials into three quantile bins (separately for conservative and liberal trials) based on pre-stimulus alpha power, such that each bin contained approximately 100 trials (Figure 3A). For the binning analyses, we mainly focused on the percentage correct (i.e., accuracy), and hit and FA rates, because these metrics scale linearly (as opposed to *d'*, which scales nonlinearly as the hit rate increases or FA rate decreases linearly) and are well defined for both behavioral data and MVPA outputs. Repeated-measures ANOVA on accuracy (priming type × α power bins) showed that pre-stimulus alpha power significantly modulated accuracy irrespective of priming type ($F_{2,56} = 3.44$, Greenhouse-Geisser corrected $p = 0.040$, $\eta_p^2 = 0.109$, $\eta_G^2 = 0.043$). Specifically, lower pre-stimulus alpha power led to higher accuracy (bin low vs. med: $t_{28} = -1.26$, $p = 0.218$; bin low vs. high: $t_{28} = 1.29$, $p = 0.208$; bin med vs. high: $t_{28} = 2.78$, $p = 0.010$). To better understand the observed accuracy results, we then repeated the same analysis on the corresponding hit and FA rates. We found that pre-stimulus alpha power significantly modulated hit rate ($F_{2,56} = 4.11$, Greenhouse-Geisser corrected $p = 0.027$, $\eta_p^2 = 0.128$, $\eta_G^2 = 0.024$), in addition to the main effect of priming type on hit rate ($F_{1,28} = 33.00$, $p < 10^{-5}$, $\eta_p^2 = 0.541$, $\eta_G^2 = 0.458$). Trials of lower pre-stimulus alpha power were associated with higher hit rate compared to those of highest pre-stimulus alpha power (bin low vs. high: $t_{28} = 2.46$, $p = 0.020$; bin med vs. high: $t_{28} = 2.18$, $p = 0.038$; bin low vs. med: $t_{28} < 1$). In contrast, we observed a similar pattern for FA rate (main effect of priming type: $F_{1,28} = 26.87$, $p < 10^{-4}$, $\eta_p^2 = 0.490$, $\eta_G^2 = 0.456$; main effect of

pre-stimulus alpha: $F_{2,56}$ = 3.47, Greenhouse-Geisser corrected p = 0.047, η_p^2 = 0.110, η_G^2 = 0.008), in which trials with the lowest pre-stimulus alpha power were associated with higher FA rate (bin low vs. med: t_{28} = 2.45, p = 0.021; bin low vs. high: t_{28} = 1.06, p = 0.300; bin med vs. high: t_{28} = -1.90, p = 0.067).

While the observed effect of pre-stimulus alpha power on accuracy suggests it modulates perceptual discriminability, the concurrent shifts in hit and FA rates hint at its role in modulating subject's decision criterion. To obtain a more fine-grained picture of the alpha power modulation of behavior, we applied generalized linear mixed models (GLMMs; see SI Methods) to account for both between-subjects and within-subject trial-by-trial response variability, and to estimate the effects of alpha oscillatory power on *d'* and criterion simultaneously. Our modeling results (Figure 3D) showed a significant negative effect of pre-stimulus alpha power on *d'*, which was exclusively driven by conservative trials (conservative: $\beta_{d'}$ = -0.0434, $p < 10^{-4}$; liberal $\beta_{d'}$ = 0.0060, p = 0.631); the effects of pre-stimulus alpha power on criterion were not statistically significant (conservative: β_c = -0.0026, p = 0.696; liberal β_c = 0.0124, p = 0.125), suggesting that the observed hit and FA rates patterns may be explained by an exclusive change in discriminability. This is, although not apparent, plausible when the hit and FA rates both increased but not to the same extent (SI Figure S3). Control analyses (SI Results) confirmed that the above reported results remain robust after removing trials in which subjects blinked during the pre-stimulus time window used to estimate alpha power. Collectively, our results indicate that pre-stimulus alpha power in visual regions most responsive to the target stimuli modulated perceptual discriminability, not criterion.

Pre-stimulus alpha power enhances sensory representation

To evaluate the quality of visual information coding, we used multi-variate pattern analysis (MVPA), operationalizing the quality of visual representation as the neural classifier's classification performance. We used the priming trials to train binary classifiers to classify target-present vs. absent trials in a time-resolved manner (SI Results), and confirmed that the classifier tracked sensory processing both qualitatively and quantitatively when applied to main task trials (SI Figure S4).

We examined whether pre-stimulus alpha power modulates the quality of visual information coding by first focusing on the neural classifier's response at the time when classification accuracy peaked (trained and tested at the time point 120 ms after stimulus onset). Similar to the above-mentioned analyses linking pre-stimulus alpha power with subject's behavior, we found that pre-stimulus alpha power modulated the representational content of neural activity (Figure 3B). Albeit the interaction effect on classification accuracy was only marginally significant ($F_{2,56}$ = 2.97, Greenhouse-Geisser corrected p = 0.059, η_p^2 = 0.096, η_G^2 = 0.031; main effect of priming: $F_{1,28}$ < 1; main effect of alpha power: $F_{2,56}$ = 1.54, p = 0.22), analyses on the classifier's hit rate indicated that lower pre-stimulus alpha power led to higher hit rate (main effects: Fs < 1; interaction: $F_{2,56}$ = 4.32, Greenhouse-Geisser corrected p = 0.020, η_p^2 = 0.134, η_G^2 = 0.045), with the modulation statistically significant only for conservative (simple main effect: $F_{2,56}$ = 4.34, Greenhouse-Geisser corrected p = 0.020; bin low vs. med, t_{28} = 2.63, p = 0.013; bin low vs. high, t_{28} = 2.46, p = 0.020; bin med vs. high, t_{28} = 0.42, p = 0.680) but not liberal (simple main effect: $F_{2,56}$ < 1) trials. We observed no statistically significant differences in the classifier's FA rate across the alpha power bins and priming types (all Fs < 1). Control analyses (SI Results) further demonstrated that these results were robust (in fact, more pronounced) after removing trials in which subjects blinked during the pre-stimulus time window used to estimate alpha power.

We also applied the GLMM to the classifier's responses and again found a negative correlation between pre-stimulus alpha power and the classifier's *d'* for both types of trials (Figure 3D, conservative: $\beta_{d'}$ = -0.0375, p = 0.012, β_c = 0.0096, p = 0.016; liberal: $\beta_{d'}$ = -0.0225, p = 0.005, β_c = -0.0031, p = 0.399), suggesting that lower pre-stimulus alpha power leads to enhanced task-relevant information coding.

In addition to examining how pre-stimulus alpha power modulated classification performance when it peaked, we asked whether the modulatory effect on classification accuracy

by pre-stimulus alpha power manifested at other time points during sensory processing. Cluster-based permutation test (on the diagonal of the temporal generalization matrix, time window = [0, 1.0] s) showed that lower pre-stimulus alpha power in the visual ROIs was associated with higher classification accuracy about 160 ms after target onset (p = 0.038, Figure 3E).

Convergingly, our classification results showed that a state of decreased pre-stimulus alpha power leads to enhanced visual representation, which likely results in better detection discriminability.

Pre-stimulus alpha power modulates *d'* predominantly in early visual areas: whole-brain analysis

While the above ROI analysis enabled us to maximize statistical power to address our research questions, it may have precluded us from observing interesting effects taking place outside our visual ROIs. To explore whether and how pre-stimulus alpha power fluctuations in different brain regions modulated subject's detection responses, we applied the GLMM analysis to all anatomical parcels, and asked whether alpha power changes in any parcel modulated the subject's *d'* or criterion. Out of many parcels showing *d'* or criterion modulation by pre-stimulus alpha power (Figure 4AB), five parcels (Figure 4C) were identified as statistically significant after controlling for false discoveries (false discovery rate 5%) due to multiple comparisons (25). While two parcels, overlapping with right frontal eye field (FEF), showed a positive *d'* modulation (i.e., higher pre-stimulus alpha power led to higher *d'*), three parcels corresponding to early visual areas showed a negative *d'* modulation (i.e., higher pre-stimulus alpha power led to lower *d'*). Interestingly, while the *d'* modulations of frontal regions were mainly driven by between-subjects variations, those of early visual areas were mainly driven by within-subject variations (SI Results). Notably, parcels in early visual areas revealed by this exploratory analysis overlapped roughly with those used in our ROI analysis, further consolidating our findings that pre-stimulus alpha activity in visual areas most responsive to the target stimuli modulated perceptual discriminability.

Pre-stimulus alpha phase modulates accuracy in a phasic manner

Finally, we asked how detection accuracy fluctuated as a function of oscillatory alpha phase. We estimated the extent of alpha phase modulation of accuracy by taking the amplitude of the fitted cosine function that best described changes of accuracy as a function of oscillatory alpha phase. We started by first examining the fitted cosine's amplitude over time during the pre-stimulus time window in the functionally-defined visual ROIs. The estimated amplitudes were significantly above chance around 200 ms before the stimulus onset, suggesting significant phasic modulation of detection accuracy (Figure 5A). Interestingly, such a phasic modulation of subject's accuracy seemingly faded out immediately before the stimulus onset. In contrast, the phasic modulation of the neural classifier's responses peaked at around 100 ms immediately before stimulus onset, suggesting that oscillatory alpha phase in these visual ROIs may have different impacts on visual representation and subject's detection responses.

Next, we asked whether any anatomical parcels exhibited significant phasic accuracy modulation by oscillatory alpha-band activity. We focused on the fitted cosine's amplitude corresponding to the time window immediately before stimulus onset whose phase estimates were unaffected by post-stimulus responses ([-0.2, -0.1] s). After correcting for multiple comparisons (false discovery rate 5%), the fitted amplitude of phasic modulation in three parcels remained statistically significant: two parcels in the parietal cortex, corresponding to the left inferior parietal gyrus and right superior parietal gyrus; and one parcel in the anterior frontal cortex (Figure 5C).

Together, these analyses of oscillatory alpha phase suggest that accuracy was modulated in a phasic manner, and that such phasic modulations are most likely driven by oscillatory alpha phase in parietal and frontal regions.

Discussion

To examine how alpha oscillations modulate perception, we recorded MEG in human subjects while they performed a visual detection task. While we successfully introduced criterion shifts in subjects' responses using the priming manipulation, such a shift was not reflected in a modulation of pre-stimulus alpha activity. We then showed that trial-by-trial fluctuations of oscillatory alpha power in early visual regions most responsive to the stimuli modulated both the subject's and neural classifier's discriminability; and that oscillatory alpha phase in parietal and anterior prefrontal areas modulated behavioral accuracy in a phasic manner.

By providing the target-presence rate and presenting clearly visible targets at the start of each block (i.e., the priming trials), we successfully changed subject's perceptual expectations and thereby introduced criterion shifts in their decisions. While recent work has demonstrated that the human brain implements perceptual expectations by activating the predicted events before the stimulus (26, 27), we did not observe any neural activity differences between the two priming conditions. Unlike a previous study where criterion was manipulated via changing the stimulus-response reward contingencies (28), our current paradigm minimized the effect of reward contingency on neural activity and arguably allowed a cleaner reconstruction of sensory responses. Moreover, we manipulated subject's perceptual expectations in a block-wise manner, therefore our null finding cannot be explained by the brain not having enough time to flexibly adjust its internal state. As indicated by the significant and sustained priming effect on behavior, subjects incorporated different perceptual expectations consistently throughout the recording session. However, these differential expectations were not reflected in pre-stimulus alpha power levels. Put differently, the endogenous shift of decision criterion does not seem to require or rely on pre-stimulus alpha modulations.

Next, we asked whether trial-by-trial fluctuations of pre-stimulus alpha oscillations lead to changes in criterion or discriminability. Using both the ROI analysis and whole-brain exploratory analysis, we showed that both the observer's perceptual discriminability and information content decodable from the neural activity patterns are enhanced when pre-stimulus alpha power in early visual areas is low. Interestingly, the modulatory effect of alpha oscillations on classification performance took place during the early stage of sensory processing (i.e., about 120–170 ms post stimulus onset), suggesting that an enhanced visual representation (29) underlies the subject's discriminability improvement in the current detection task. Collectively, these results support the multiplicative hypothesis, i.e., that lower pre-stimulus alpha power amplifies the neural response such that the signal of interest becomes more distinct from noise, thereby improving perceptual discriminability.

The fact that we observed no significant differences in pre-stimulus alpha power between different priming conditions, and that we found little criterion modulation by trial-by-trial pre-stimulus alpha power change, should, however, be interpreted with caution: Not only because the absence of evidence is not evidence of absence, but also because a discriminability change in the true generative model almost always leads to both discriminability and criterion changes in the observed behavior (21). For the latter reason, the existing relationship between alpha oscillations and discriminability may have undermined our statistical power of observing any significant criterion modulation by alpha oscillations, as experimenters can only infer the observer's internal response distribution from her responses. Furthermore, it is noteworthy that, unlike conventional detection paradigms in which no stimuli are presented on target-absent trials and sensory uncertainty is controlled by directly adjusting the amount of sensory information in task-relevant stimuli (e.g., contrast of the visual target), we presented noise patches in target-absent trials, and introduced sensory uncertainty by adjusting the strength of the task-irrelevant backward masks. Below, we highlight how these rather unconventional experimental manipulations may provide critical insights to our question of interest.

First, presenting noise patches on target-absent trials allowed us to always unequivocally define the pre-stimulus window of interest. This is distinct from previous studies using a conventional detection paradigm with pre-stimulus windows of variable duration. Because in that case no stimulus is presented on target-absent trials, there is no stimulus onset to reference to, which makes the definition of the "pre-stimulus" window rather arbitrary. Arguably, this can be easily reconciled if the stimulus onset is made predictable to the subject (e.g., by using temporal

cues and fixed pre-stimulus windows). However, the immediate question is to what extent top-down processes contribute to pre-stimulus alpha oscillations recorded using such paradigms. Indeed, previous work has shown that human subjects endogenously adjusted the oscillatory alpha state (both in terms of power (30) and phase (31)) prior to the predictable onset of relevant stimuli to optimize sensory processing, suggesting that such paradigms may capture different neural dynamics than ours.

Second, introducing sensory uncertainty via backward masking enabled us to display our stimuli of interest in high contrast, thereby boosting the signal-to-noise ratio in the corresponding neural signals. This further allowed us to reliably classify neural activity patterns of interest, which offered a unique opportunity to directly test whether and how alpha oscillations shape information coding. Moreover, it has been suggested that backward masking interrupts recurrent processes essential to conscious perception (32, 33). Two temporally dissociable recurrent processes involved in conscious visual perception have been identified: (*i*) the local recurrent process, which occurs involuntarily within the ventral visual stream about 150 ms after stimulus onset, and (*ii*) the top-down recurrent process, which originates from frontal and parietal regions about 200 ms after stimulus onset with voluntary attention (for a review of the temporal dynamics, see (34)). Both processes play important roles in maintaining task-relevant neural activity over time. Here, we found that the modulatory effect of pre-stimulus alpha power on classification performance was strongest around 160 ms after stimulus onset, during which the local recurrent process dominates. The current results suggest that lower oscillatory alpha power reflects enhanced local recurrent processing. This proposal is speculative, however, and in need of further empirical evidence.

Finally, having demonstrated the relationship between alpha power and perception, we asked whether pre-stimulus alpha modulates behavioral accuracy in a phasic manner, as predicted by the inhibition hypothesis (4, 5, 35). We found that alpha phase immediately prior to stimulus onset in parietal and anterior frontal areas—but not in visual areas—modulated subject's accuracy. While one may expect the alpha phase effect to be dependent on and additive to the alpha power effect (36), our findings are consistent with previous work showing that alpha phase and power effects have different spatial topographies (37). While not the focus of the current study, further research is needed to understand how the interplay between oscillatory alpha power and phase modulates perception.

To summarize, the current study shows with complementary uni- and multi-variate results that changes of pre-stimulus alpha-band power modulate the quality of visual information coding at the neural level and perceptual discriminability at the behavioral level. These findings provide important insights into how ongoing neural activity sets the internal state and subsequently influences perception.

Materials and Methods

Subjects

Thirty-four healthy volunteers completed the full experiment. Two of them were excluded from analysis because of excessive head movement during the MEG recording, resulting in the planned sample size of 32 subjects in the reported analysis (mean age = 25.8, SD = 6.0; 23 females). The study was approved by the local ethics committee (CMO Arnhem-Nijmegen). All subjects gave informed consent prior to the experiment and received monetary compensation for their participation.

Procedure

Subjects reported to the lab on two days within one week, for a training session on day 1 and MEG recording session on day 2 (SI Procedure).

Main experimental block. Two stimuli, a target and a mask, were presented sequentially in each trial (SI Stimuli), and the subject's task was to report as accurately as possible whether a grating was present or not in the trial (see Figure 2A for trial schematic). To introduce criterion shift in

subject's perceptual decisions, we designed a paradigm inspired by Crapse and colleagues (38). Each main experimental block started with an instruction screen, informing subjects of the orientation (CW or CCW) and grating presence rate (20% or 80%) in the upcoming block. Every block consisted of 40 priming trials and 80 main task trials. For the first 40 priming trials, gratings were presented either 20% or 80% of the time, consistent with the block instruction. The backward masks were of 5% Michelson contrast, which had little masking effect on the target grating. We purposely presented the targets in a clearly discriminable way during the priming phase, to encourage subjects to shift their decision criteria accordingly. Before starting the 80 main task trials, a reminder was presented on the screen for three seconds, highlighting the current block's target orientation and presence rate again. From the subject's point of view, other than a contrast increase in the backward mask (titrated for each subject), everything remained the same between priming and main task trials. However, unbeknownst to the subjects, gratings were presented 50% of the time irrespective of the instructed target presence rate (and contrary to the priming part of the block). Critically, the increased perceptual ambiguity due to strong backward masks allowed us to keep grating presence rate the same between conservative and liberal priming blocks, while introducing a bias in subject's perceptual decisions.

Grating localizer block. Interleaved with the main task blocks, subjects performed three blocks of a grating localizer task (see Figure 2A for trial schematic). Each block consisted of 120 trials, among which 18 trials contained a brief fixation blink (i.e., the central fixation dot turned from black to white for 50 ms). The subject's task was to detect these occasional fixation blinks and to press a button as soon as possible when they saw them. Clockwise and counterclockwise gratings identical to those presented during the main task were presented in a pseudorandom order for 250 ms, followed by a uniformly jittered ITI of 1 to 1.5 s. We used a longer presentation duration (relative to that used in the main task trials) to increase the signal-to-noise ratio in the stimulus-driven response. These trials enabled us to identify brain regions most responsive to the bottom-up stimulation by grating stimuli. Trials containing fixation blinks—which served exclusively to maintain the subject's attention on the fixation point—were excluded from later analyses.

Behavioral Data

We focused our analysis on main task trials (i.e., trials with high-contrast backward masks) recoded during the MEG session. Besides accuracy and reaction times (RT), our main behavioral variables of interest were discriminability (*d'*) and criterion (*c*), which were estimated following Signal Detection Theory (SDT), assuming the internal signal and noise distributions shared the same variance (21) as follows:

$$d' = z(Hit) - z(FA) \text{ (Equation 1)}$$

$$c = -\frac{1}{2}(z(Hit) + z(FA)) \text{ (Equation 2)}$$

We used the Wilcoxon signed-rank test on *d'* and criterion, and the within-subject repeated-measures ANOVA (priming type: conservative vs. liberal; grating orientation: clockwise vs. counter-clockwise) on accuracy and correct RTs to assess the effect of priming on behavior.

To link our neural data with behavioral data, we grouped the trials into quantile bins based on the neural data of interest (e.g., pre-stimulus alpha power), and applied a within-subject repeated-measures ANOVA to investigate whether and how behavioral measures differ across quantile bins of the neural variable of interest. We additionally reported partial eta squared (η_p) and generalized eta squared (η_G), as recommended by Lakens (39) to facilitate meta-analysis on similar studies.

Moreover, for a more fine-grained analysis of the relationship between pre-stimulus oscillatory alpha power and behavioral outcomes, we adapted and extended the Generalized Linear Model (GLM) formulation of SDT (40) to capitalize on both between-subjects and within-subject trial-by-trial fluctuations (SI Generalized linear mixed model). We pooled trial data from all subjects, constructed a hierarchical model and estimated population-level parameters $\beta_{d'}$ and β_c denoting the effect of pre-stimulus oscillatory alpha power on discriminability and criterion. A negative value of $\beta_{d'}$ (or β_c) indicates that *d'* (or criterion) decreases as pre-stimulus oscillatory

alpha power increases. Similarly, to evaluate whether accuracy was modulated in a phasic manner, we binned trials based on the oscillatory alpha phase and modelled the accuracy scores of each phase bin using cosine functions. We indexed the amount of phasic accuracy modulation using the amplitude of the fitted cosine function (see SI Phasic modulation of accuracy). Intuitively, an estimated amplitude of 3% suggested that the model predicted an accuracy difference of 6% between trials of the optimal phase and those of the suboptimal phase.

MEG Data

Brain activity was recorded using a 275-channel axial gradiometer MEG system (CTF MEG Systems, VSM MedTech Ltd) at 1200 Hz in a magnetically shielded room. Three fiducial coils were placed at the subject's nasion and both ear canals, to provide online monitoring (41) of the subject's head position and to serve as anatomical landmarks for offline co-registration with structural MRI scans (SI Data acquisition).

MEG data were pre-processed offline and analyzed using the FieldTrip toolbox (41) and custom-built Matlab scripts (SI MEG preprocessing). Event-related fields were computed and transformed to planar gradients, to make interpretation of the sensor-level data easier and to facilitate the comparison of ERF topographies across subjects (SI Event-related fields).

Source-level analyses reported in the results section are based on a sample of 29 subjects, whose T1-weighted anatomical images were available for creating subject-specific source and volume conduction models (SI MRI preprocessing). Source-level estimates of the time domain data were modelled on cortically constrained meshes of dipole positions using the linearly constrained maximum variance (LCMV) beamformer approach (42). Neural response time series of an anatomical parcel (defined by the Conte69 atlas (43)) were computed by taking the first principal component of the time series over all dipole positions within the parcel. The partial canonical coherence beamformer approach (44) was used to localize the sources of oscillatory activity in response to the main task trials (SI Source reconstruction).

Time-frequency representations (TFRs) of power were calculated for each trial by applying a fast Fourier transform to short sliding time windows. We applied Hanning tapers of 4-cycles length in time steps of 50 ms to single-trial data, prior to computing the spectra (4–30 Hz). For sensor-level analyses, spectral decomposition was applied to synthetic planar gradient data, and combined into single spectra per sensor. Condition-average TFRs were expressed relative to a frequency-specific baseline window, which started 4 cycles and ended 2 cycles before stimulus onset (e.g., for 10-Hz activity, a 400 to 200 ms pre-stimulus time window was used as baseline window) to prevent leakage of post-stimulus activity into the baseline window. To compute TFRs of an anatomical parcel (source-level), spectral decomposition was performed on the parcel's response time series (SI Source reconstruction). To estimate the time courses of oscillatory alpha phase, we used Hanning tapers of 2-cycles length at 10 Hz, to slide over each anatomical parcel's response time series in steps of 5 ms. The phase was computed as the angle of the resulting Fourier coefficients.

To probe the representational content of neural activity, we performed multivariate pattern analysis using the MVPA-light toolbox (45). Before running the classification analysis, we first applied a low-pass filter at 30 Hz and down-sampled the data to 100 Hz. Multivariate logistic regression (L2 regularized) was then applied to predict the grating's presence (present vs. absent), based on the sensor-level spatial distribution of neural activity at each time point. To avoid overfitting, we trained the classifier with priming trials, and tested on the main task trials. This procedure was done within-subject in a time-resolved manner, resulting in a temporal generalization matrix (46).

Statistical analyses were conducted using cluster-based permutation tests ((47), see SI Cluster-based permutation test).

Acknowledgments

We thank Kristina Baumgart and Felix Linsen for their assistance with data acquisition. This study was supported by the Netherlands Organization for Scientific Research Vidi grants (NWO 016.Vidi.185.137 awarded to SH, and 864.14.011 to JMS), the Chinese Scholarship Council (CSC20170800036 awarded to YJZ), and the European Union Horizon 2020 Program (ERC Starting Grant 678286, "Contextvision" awarded to FPdL).

References

1. J. Samaha, L. Iemi, S. Haegens, N. A. Busch, Spontaneous Brain Oscillations and Perceptual Decision-Making. *Trends in Cognitive Sciences* **24**, 639–653 (2020).

2. K. D. Harris, A. Thiele, Cortical state and attention. *Nature Reviews Neuroscience* **12**, 509–523 (2011).

3. H. Berger, Über das Elektrenkephalogramm des Menschen. *Archiv für Psychiatrie und Nervenkrankheiten* **87**, 527–570 (1929).

4. O. Jensen, A. Mazaheri, Shaping functional architecture by oscillatory alpha activity: Gating by inhibition. *Frontiers in Human Neuroscience* **4** (2010).

5. W. Klimesch, P. Sauseng, S. Hanslmayr, EEG alpha oscillations: The inhibition-timing hypothesis. *Brain Research Reviews* **53**, 63–88 (2007).

6. O. Jensen, M. Bonnefond, R. VanRullen, An oscillatory mechanism for prioritizing salient unattended stimuli. *Trends in Cognitive Sciences* **16**, 200–206 (2012).

7. S. Haegens, V. Nácher, R. Luna, R. Romo, O. Jensen, α-Oscillations in the monkey sensorimotor network influence discrimination performance by rhythmical inhibition of neuronal spiking. *Proceedings of the National Academy of Sciences of the United States of America* **108**, 19377–19382 (2011).

8. E. Spaak, M. Bonnefond, A. Maier, D. A. Leopold, O. Jensen, Layer-specific entrainment of gamma-band neural activity by the alpha rhythm in monkey visual cortex. *Current Biology* (2012) https:/doi.org/10.1016/j.cub.2012.10.020.

9. R. Scheeringa, *et al.*, Neuronal Dynamics Underlying High- and Low-Frequency EEG Oscillations Contribute Independently to the Human BOLD Signal. *Neuron* **69**, 572–583 (2011).

10. V. Romei, *et al.*, Spontaneous fluctuations in posterior α-band EEG activity reflect variability in excitability of human visual areas. *Cerebral Cortex* **18**, 2010–2018 (2008).

11. D. Osipova, D. Hermes, O. Jensen, Gamma power is phase-locked to posterior alpha activity. *PLoS ONE* **3** (2008).

12. R. Scheeringa, A. Mazaheri, I. Bojak, D. G. Norris, A. Kleinschmidt, Modulation of visually evoked cortical fMRI responses by phase of ongoing occipital alpha oscillations. *Journal of Neuroscience* **31**, 3813–3820 (2011).

13. L. Dugué, P. Marque, R. VanRullen, The phase of ongoing oscillations mediates the causal relation between brain excitation and visual perception. *Journal of Neuroscience* **31**, 11889–11893 (2011).

14. F. van Ede, F. de Lange, O. Jensen, E. Maris, Orienting attention to an upcoming tactile event involves a spatially and temporally specific modulation of sensorimotor alpha- and beta-band oscillations. *Journal of Neuroscience* **31**, 2016–2024 (2011).

15. S. Haegens, B. F. Händel, O. Jensen, Top-down controlled alpha band activity in somatosensory areas determines behavioral performance in a discrimination task. *Journal of Neuroscience* **31**, 5197–5204 (2011).

16. G. Thut, A. Nietzel, S. A. Brandt, A. Pascual-Leone, α-Band electroencephalographic activity over occipital cortex indexes visuospatial attention bias and predicts visual target detection. *Journal of Neuroscience* **26**, 9494–9502 (2006).

17. H. van Dijk, J. M. Schoffelen, R. Oostenveld, O. Jensen, Prestimulus oscillatory activity in the alpha band predicts visual discrimination ability. *Journal of Neuroscience* **28**, 1816–1823 (2008).

18. S. Hanslmayr, *et al.*, Prestimulus oscillations predict visual perception performance between and within subjects. *NeuroImage* **37**, 1465–1473 (2007).

19. L. Iemi, M. Chaumon, S. M. Crouzet, N. A. Busch, Spontaneous Neural Oscillations Bias Perception by Modulating Baseline Excitability. *The Journal of Neuroscience* **37**, 807–819 (2017).

20. J. Samaha, L. Iemi, B. R. Postle, Prestimulus alpha-band power biases visual discrimination confidence, but not accuracy. *Consciousness and Cognition* **54**, 47–55 (2017).

21. N. A. Macmillan, C. D. Creelman, *Detection Theory: A User's Guide: 2nd edition* (2004) https:/doi.org/10.4324/9781410611147.

22. C. S. Y. Benwell, *et al.*, Prestimulus EEG power predicts conscious awareness but not objective visual performance. *eNeuro* **4** (2017).

23. K. Limbach, P. M. Corballis, Prestimulus alpha power influences response criterion in a detection task. *Psychophysiology* **53**, 1154–1164 (2016).

24. R. B. Mars, *et al.*, Trial-by-trial fluctuations in the event-related electroencephalogram reflect dynamic changes in the degree of surprise. *Journal of Neuroscience* **28**, 12539–12545 (2008).

25. Y. Benjamini, Y. Hochberg, On the adaptive control of the false discovery rate in multiple testing with independent statistics. *Journal of Educational and Behavioral Statistics* **25**, 60–83 (2000).

26. P. Kok, P. Mostert, F. P. de Lange, Prior expectations induce prestimulus sensory templates. *Proceedings of the National Academy of Sciences of the United States of America* **114**, 10473–10478 (2017).

27. M. Ekman, P. Kok, F. P. de Lange, Time-compressed preplay of anticipated events in human primary visual cortex. *Nature Communications* **8** (2017).

28. N. A. Kloosterman, *et al.*, Humans strategically shift decision bias by flexibly adjusting sensory evidence accumulation. *eLife* **8** (2019).

29. P. Kok, J. F. M. Jehee, F. P. de Lange, Less Is More: Expectation Sharpens Representations in the Primary Visual Cortex. *Neuron* **75**, 265–270 (2012).

30. G. Rohenkohl, A. C. Nobre, Alpha oscillations related to anticipatory attention follow temporal expectations. *Journal of Neuroscience* **31**, 14076–14084 (2011).

31. J. Samaha, P. Bauer, S. Cimaroli, B. R. Postle, Top-down control of the phase of alpha-band oscillations as a mechanism for temporal prediction. *Proceedings of the National Academy of Sciences of the United States of America* **112**, 8439–8444 (2015).

32. S. Dehaene, J. P. Changeux, L. Naccache, J. Sackur, C. Sergent, Conscious, preconscious, and subliminal processing: a testable taxonomy. *Trends in Cognitive Sciences* **10**, 204–211 (2006).

33. V. A. F. Lamme, P. R. Roelfsema, The distinct modes of vision offered by feedforward and recurrent processing. *Trends in Neurosciences* **23**, 571–579 (2000).

34. D. Wyatte, D. J. Jilk, R. C. O'Reilly, Early recurrent feedback facilitates visual object recognition under challenging conditions. *Frontiers in Psychology* **5** (2014).

35. K. E. Mathewson, *et al.*, Pulsed out of awareness: EEG alpha oscillations represent a pulsed-inhibition of ongoing cortical processing. *Frontiers in Psychology* **2** (2011).

36. K. E. Mathewson, G. Gratton, M. Fabiani, D. M. Beck, T. Ro, To see or not to see: Prestimulus α phase predicts visual awareness. *Journal of Neuroscience* **29**, 2725–2732 (2009).

37. N. A. Busch, R. VanRullen, Spontaneous EEG oscillations reveal periodic sampling of visual attention. *Proceedings of the National Academy of Sciences of the United States of America* **107**, 16048–16053 (2010).

38. T. B. Crapse, H. Lau, M. A. Basso, A Role for the Superior Colliculus in Decision Criteria. *Neuron* **97**, 181-194.e6 (2018).

39. D. Lakens, Calculating and reporting effect sizes to facilitate cumulative science: A practical primer for t-tests and ANOVAs. *Frontiers in Psychology* **4** (2013).

40. L. T. DeCarlo, Signal Detection Theory and Generalized Linear Models. *Psychological Methods* **3**, 186–205 (1998).

41. R. Oostenveld, P. Fries, E. Maris, J. M. Schoffelen, FieldTrip: Open source software for advanced analysis of MEG, EEG, and invasive electrophysiological data. *Computational Intelligence and Neuroscience* **2011**, 1–9 (2011).

42. B. D. van Veen, W. van Drongelen, M. Yuchtman, A. Suzuki, Localization of brain electrical activity via linearly constrained minimum variance spatial filtering. *IEEE Transactions on Biomedical Engineering* **44**, 867–880 (1997).

43. D. C. van Essen, M. F. Glasser, D. L. Dierker, J. Harwell, T. Coalson, Parcellations and hemispheric asymmetries of human cerebral cortex analyzed on surface-based atlases. *Cerebral Cortex* (2012) https:/doi.org/10.1093/cercor/bhr291.

44. J. M. Schoffelen, R. Oostenveld, P. Fries, Imaging the human motor system's beta-band synchronization during isometric contraction. *NeuroImage* **41**, 437–447 (2008).

45. M. S. Treder, MVPA-Light: A Classification and Regression Toolbox for Multi-Dimensional Data. *Frontiers in Neuroscience* **14** (2020).

46. J. R. King, S. Dehaene, Characterizing the dynamics of mental representations: The temporal generalization method. *Trends in Cognitive Sciences* **18**, 203–210 (2014).

47. E. Maris, R. Oostenveld, Nonparametric statistical testing of EEG- and MEG-data. *Journal of Neuroscience Methods* **164**, 177–190 (2007).

1. J. Samaha, L. Iemi, S. Haegens, N. A. Busch, Spontaneous Brain Oscillations and Perceptual Decision-Making. *Trends in Cognitive Sciences* **24**, 639–653 (2020).

2. K. D. Harris, A. Thiele, Cortical state and attention. *Nature Reviews Neuroscience* **12**, 509–523 (2011).

3. H. Berger, Über das Elektrenkephalogramm des Menschen. *Archiv für Psychiatrie und Nervenkrankheiten* **87**, 527–570 (1929).

4. O. Jensen, A. Mazaheri, Shaping functional architecture by oscillatory alpha activity: Gating by inhibition. *Frontiers in Human Neuroscience* **4** (2010).

5. W. Klimesch, P. Sauseng, S. Hanslmayr, EEG alpha oscillations: The inhibition-timing hypothesis. *Brain Research Reviews* **53**, 63–88 (2007).

6. O. Jensen, M. Bonnefond, R. VanRullen, An oscillatory mechanism for prioritizing salient unattended stimuli. *Trends in Cognitive Sciences* **16**, 200–206 (2012).

7. S. Haegens, V. Nácher, R. Luna, R. Romo, O. Jensen, α-Oscillations in the monkey sensorimotor network influence discrimination performance by rhythmical inhibition of neuronal spiking. *Proceedings of the National Academy of Sciences of the United States of America* **108**, 19377–19382 (2011).

8. E. Spaak, M. Bonnefond, A. Maier, D. A. Leopold, O. Jensen, Layer-specific entrainment of gamma-band neural activity by the alpha rhythm in monkey visual cortex. *Current Biology* (2012) https:/doi.org/10.1016/j.cub.2012.10.020.

9. R. Scheeringa, *et al.*, Neuronal Dynamics Underlying High- and Low-Frequency EEG Oscillations Contribute Independently to the Human BOLD Signal. *Neuron* **69**, 572–583 (2011).

10. V. Romei, *et al.*, Spontaneous fluctuations in posterior α-band EEG activity reflect variability in excitability of human visual areas. *Cerebral Cortex* **18**, 2010–2018 (2008).

11. D. Osipova, D. Hermes, O. Jensen, Gamma power is phase-locked to posterior alpha activity. *PLoS ONE* **3** (2008).

12. R. Scheeringa, A. Mazaheri, I. Bojak, D. G. Norris, A. Kleinschmidt, Modulation of visually evoked cortical fMRI responses by phase of ongoing occipital alpha oscillations. *Journal of Neuroscience* **31**, 3813–3820 (2011).

13. L. Dugué, P. Marque, R. VanRullen, The phase of ongoing oscillations mediates the causal relation between brain excitation and visual perception. *Journal of Neuroscience* **31**, 11889–11893 (2011).

14. F. van Ede, F. de Lange, O. Jensen, E. Maris, Orienting attention to an upcoming tactile event involves a spatially and temporally specific modulation of sensorimotor alpha- and beta-band oscillations. *Journal of Neuroscience* **31**, 2016–2024 (2011).

15. S. Haegens, B. F. Händel, O. Jensen, Top-down controlled alpha band activity in somatosensory areas determines behavioral performance in a discrimination task. *Journal of Neuroscience* **31**, 5197–5204 (2011).

16. G. Thut, A. Nietzel, S. A. Brandt, A. Pascual-Leone, α-Band electroencephalographic activity over occipital cortex indexes visuospatial attention bias and predicts visual target detection. *Journal of Neuroscience* **26**, 9494–9502 (2006).

17. H. van Dijk, J. M. Schoffelen, R. Oostenveld, O. Jensen, Prestimulus oscillatory activity in the alpha band predicts visual discrimination ability. *Journal of Neuroscience* **28**, 1816–1823 (2008).

18. S. Hanslmayr, *et al.*, Prestimulus oscillations predict visual perception performance between and within subjects. *NeuroImage* **37**, 1465–1473 (2007).

19. L. Iemi, M. Chaumon, S. M. Crouzet, N. A. Busch, Spontaneous Neural Oscillations Bias Perception by Modulating Baseline Excitability. *The Journal of Neuroscience* **37**, 807–819 (2017).

20. J. Samaha, L. Iemi, B. R. Postle, Prestimulus alpha-band power biases visual discrimination confidence, but not accuracy. *Consciousness and Cognition* **54**, 47–55 (2017).

21. N. A. Macmillan, C. D. Creelman, *Detection Theory: A User's Guide: 2nd edition* (2004) https:/doi.org/10.4324/9781410611147.

22. C. S. Y. Benwell, *et al.*, Prestimulus EEG power predicts conscious awareness but not objective visual performance. *eNeuro* **4** (2017).

23. K. Limbach, P. M. Corballis, Prestimulus alpha power influences response criterion in a detection task. *Psychophysiology* **53**, 1154–1164 (2016).

24. R. B. Mars, *et al.*, Trial-by-trial fluctuations in the event-related electroencephalogram reflect dynamic changes in the degree of surprise. *Journal of Neuroscience* **28**, 12539–12545 (2008).

25. Y. Benjamini, Y. Hochberg, On the adaptive control of the false discovery rate in multiple testing with independent statistics. *Journal of Educational and Behavioral Statistics* **25**, 60–83 (2000).

26. P. Kok, P. Mostert, F. P. de Lange, Prior expectations induce prestimulus sensory templates. *Proceedings of the National Academy of Sciences of the United States of America* **114**, 10473–10478 (2017).

27. M. Ekman, P. Kok, F. P. de Lange, Time-compressed preplay of anticipated events in human primary visual cortex. *Nature Communications* **8** (2017).

28. N. A. Kloosterman, *et al.*, Humans strategically shift decision bias by flexibly adjusting sensory evidence accumulation. *eLife* **8** (2019).

29. P. Kok, J. F. M. Jehee, F. P. de Lange, Less Is More: Expectation Sharpens Representations in the Primary Visual Cortex. *Neuron* **75**, 265–270 (2012).

30. G. Rohenkohl, A. C. Nobre, Alpha oscillations related to anticipatory attention follow temporal expectations. *Journal of Neuroscience* **31**, 14076–14084 (2011).

31. J. Samaha, P. Bauer, S. Cimaroli, B. R. Postle, Top-down control of the phase of alpha-band oscillations as a mechanism for temporal prediction. *Proceedings of the National Academy of Sciences of the United States of America* **112**, 8439–8444 (2015).

32. S. Dehaene, J. P. Changeux, L. Naccache, J. Sackur, C. Sergent, Conscious, preconscious, and subliminal processing: a testable taxonomy. *Trends in Cognitive Sciences* **10**, 204–211 (2006).

33. V. A. F. Lamme, P. R. Roelfsema, The distinct modes of vision offered by feedforward and recurrent processing. *Trends in Neurosciences* **23**, 571–579 (2000).

34. D. Wyatte, D. J. Jilk, R. C. O'Reilly, Early recurrent feedback facilitates visual object recognition under challenging conditions. *Frontiers in Psychology* **5** (2014).

35. K. E. Mathewson, *et al.*, Pulsed out of awareness: EEG alpha oscillations represent a pulsed-inhibition of ongoing cortical processing. *Frontiers in Psychology* **2** (2011).

36. K. E. Mathewson, G. Gratton, M. Fabiani, D. M. Beck, T. Ro, To see or not to see: Prestimulus α phase predicts visual awareness. *Journal of Neuroscience* **29**, 2725–2732 (2009).

37. N. A. Busch, R. VanRullen, Spontaneous EEG oscillations reveal periodic sampling of visual attention. *Proceedings of the National Academy of Sciences of the United States of America* **107**, 16048–16053 (2010).

38. T. B. Crapse, H. Lau, M. A. Basso, A Role for the Superior Colliculus in Decision Criteria. *Neuron* **97**, 181-194.e6 (2018).

39. D. Lakens, Calculating and reporting effect sizes to facilitate cumulative science: A practical primer for t-tests and ANOVAs. *Frontiers in Psychology* **4** (2013).

40. L. T. DeCarlo, Signal Detection Theory and Generalized Linear Models. *Psychological Methods* **3**, 186–205 (1998).

41. R. Oostenveld, P. Fries, E. Maris, J. M. Schoffelen, FieldTrip: Open source software for advanced analysis of MEG, EEG, and invasive electrophysiological data. *Computational Intelligence and Neuroscience* **2011**, 1–9 (2011).

42. B. D. van Veen, W. van Drongelen, M. Yuchtman, A. Suzuki, Localization of brain electrical activity via linearly constrained minimum variance spatial filtering. *IEEE Transactions on Biomedical Engineering* **44**, 867–880 (1997).

43. D. C. van Essen, M. F. Glasser, D. L. Dierker, J. Harwell, T. Coalson, Parcellations and hemispheric asymmetries of human cerebral cortex analyzed on surface-based atlases. *Cerebral Cortex* (2012) https:/doi.org/10.1093/cercor/bhr291.

44. J. M. Schoffelen, R. Oostenveld, P. Fries, Imaging the human motor system's beta-band synchronization during isometric contraction. *NeuroImage* **41**, 437–447 (2008).

45. M. S. Treder, MVPA-Light: A Classification and Regression Toolbox for Multi-Dimensional Data. *Frontiers in Neuroscience* **14** (2020).

46. J. R. King, S. Dehaene, Characterizing the dynamics of mental representations: The temporal generalization method. *Trends in Cognitive Sciences* **18**, 203–210 (2014).

47. E. Maris, R. Oostenveld, Nonparametric statistical testing of EEG- and MEG-data. *Journal of Neuroscience Methods* **164**, 177–190 (2007).

Figures and Tables

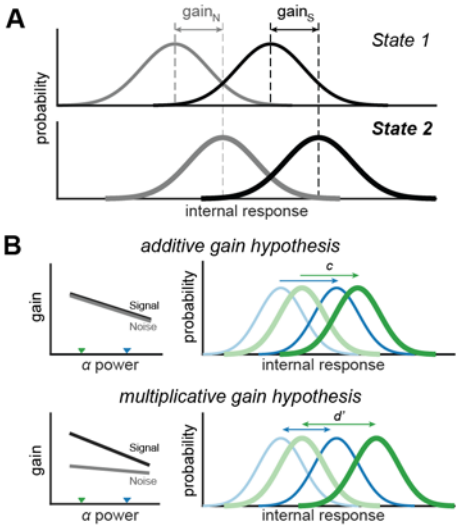

Figure 1. Hypothesis schematic. (A) Internal response distribution in different states, with state 1 the initial or baseline state (internal response distribution of signal modeled as a normal distribution with mean $\mu_{signal1}$ and standard deviation σ_1, and that of noise as μ_{noise1} and σ_1). We defined gain as $g_{signal} = \frac{\mu_{signal2} - \mu_{signal1}}{\sqrt{\sigma_1^2 + \sigma_2^2}}$ for the signal distributions, and $g_{noise} = \frac{\mu_{noise2} - \mu_{noise1}}{\sqrt{\sigma_1^2 + \sigma_2^2}}$ for the noise distributions. We set $\sigma_1 = \sigma_2$ here for simplicity. **(B)** Both models assume that response gain decreases as alpha power increases. The additive hypothesis predicts that the difference in response gain between signal and noise distributions remains constant across different alpha power levels, and therefore predicts a criterion shift when comparing two states of different alpha power (denoted by the triangles in the left panel). In contrast, the multiplicative hypothesis predicts that the difference in response gain scales as a function of alpha power, and therefore predicts a *d'* change when comparing two states of different alpha power.

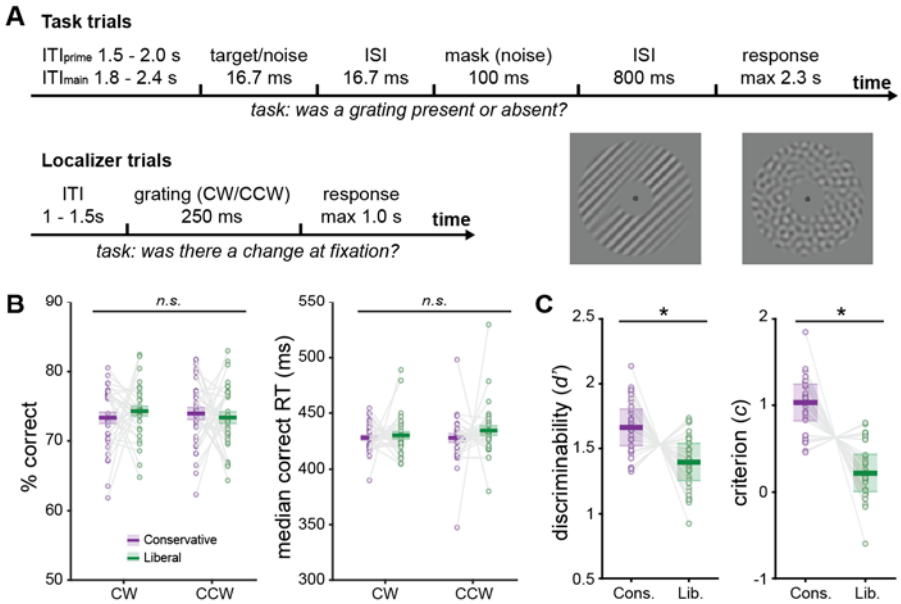

Figure 2. Experimental paradigm and behavioral results. (A) Schematic of the task trials (upper panel) and localizer trials (lower panel). Example grating and noise stimuli are shown for illustration purposes. **(B)** Accuracy and reaction times and **(C)** discriminability and criterion for the main task trials during the MEG recording. Shaded areas denote within-subject standard errors in (B), and the 25% and 75% quantiles in (C). Dots represent individual subjects (N=32). Asterisk denotes statistical significance ($p < 0.05$).

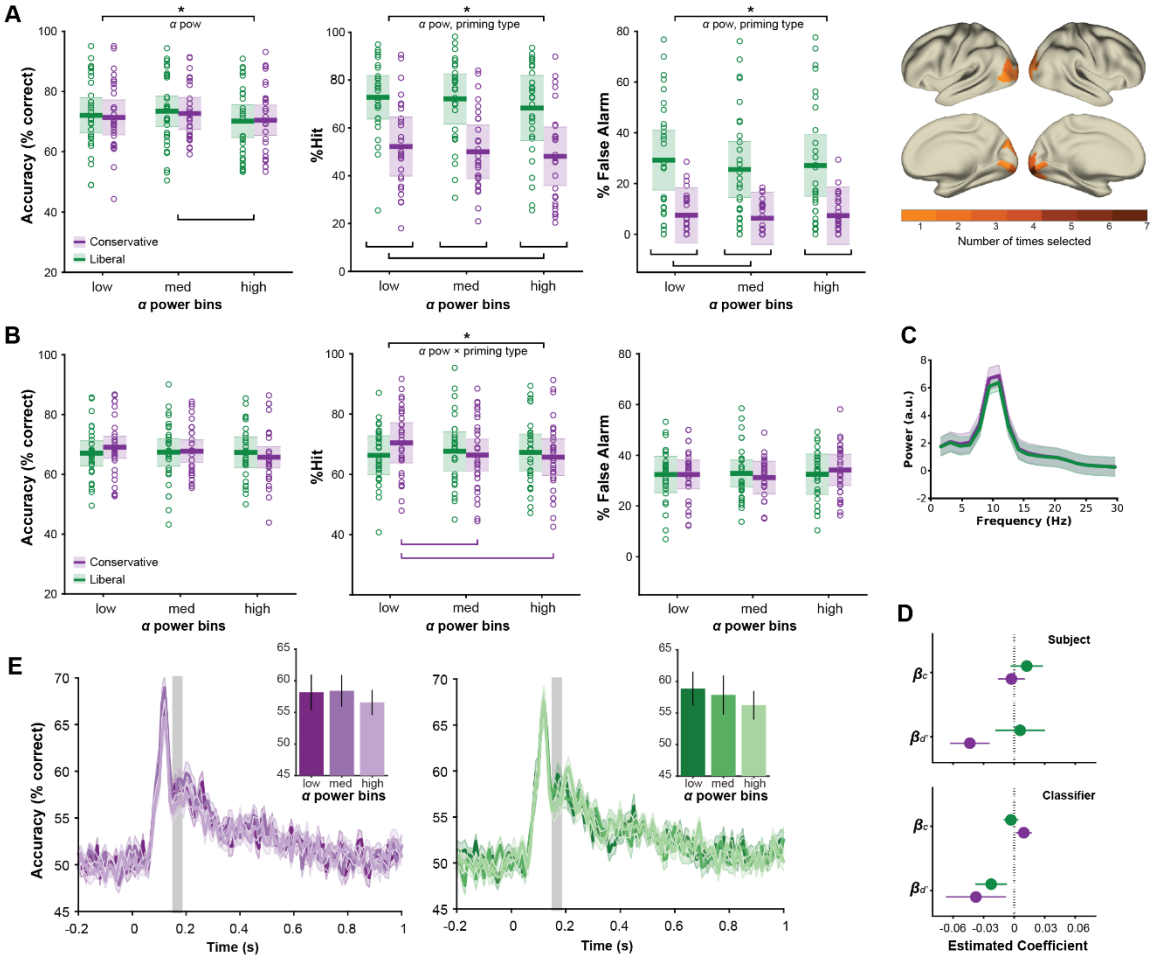

Figure 3. ROI-based analysis of relationship between alpha and performance. **(A)** Subjects' accuracy (left), hit rate (middle), and false alarm rate (right) as a function of alpha power. Parcels selected for these analyses are highlighted in the brain plots on the right. Shaded areas denote within-subject standard errors. Dots represent individual subjects. Asterisk denotes statistical significance ($p < 0.05$). **(B)** The classifier's classification accuracy (left), hit rate (middle), and false alarm rate (right) as a function of alpha power. **(C)** Power spectrum of the pre-stimulus time window [-0.5, 0] s. **(D)** Estimated coefficients and the corresponding 95% confidence intervals from the GLMM analysis. **(E)** Decoding accuracy (diagonal of the temporal generalization matrix) as a function of pre-stimulus alpha power for conservative (left) and liberal (right) trials. Gray shaded area marks the time window during which pre-stimulus alpha power significantly modulated decoding accuracy indicated by the corresponding cluster-based permutation test. Shaded area around the time series denotes within-subject standard error. Bar graphs show mean decoding accuracy averaged across the significant time points as a function of pre-stimulus alpha power. Error bars denote within-subject standard error.

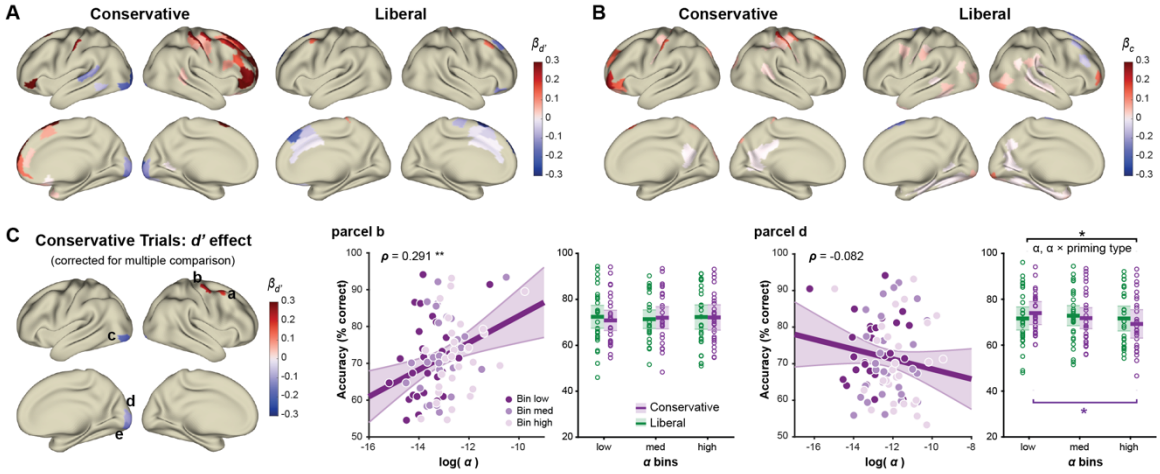

Figure 4. Whole-brain GLMM analysis of relationship between alpha and performance. **(A)** Estimated for conservative and liberal trials (masked by statistical significance of the estimated coefficients, uncorrected for multiple comparisons). **(B)** Similar to (A), estimated for conservative and liberal trials. **(C)** Estimated for conservative trials, masked by statistical significance after correction of multiple comparisons. For each parcel (labeled in the brain plot), both between-subjects correlation of accuracy and alpha power, and within-subject comparison of accuracy as a function of alpha power are shown. Results correspond to analyses in which trials with eye blinks during the pre-stimulus time interval of interest were excluded. Shaded areas denote within-subject standard errors. Dots represent individual subjects. Asterisk denotes statistical significance ($p < 0.05$).

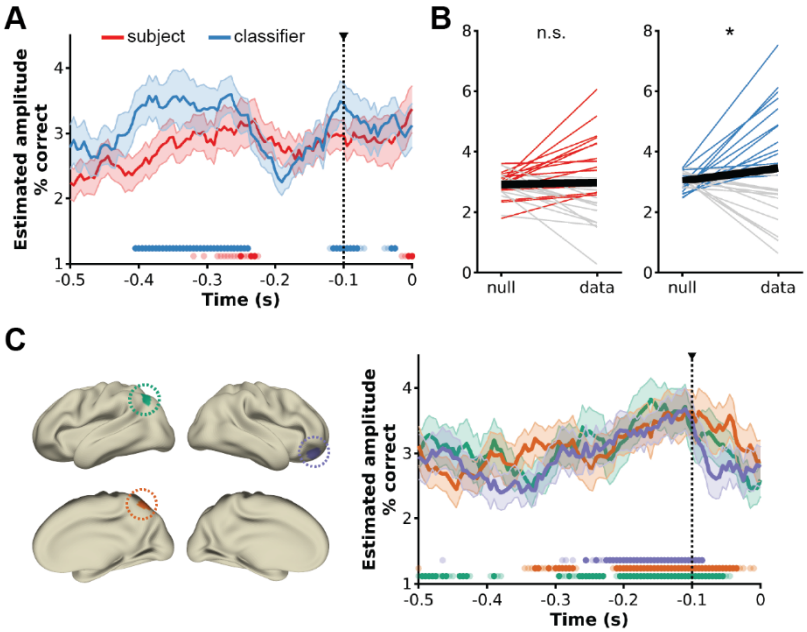

Figure 5. Phasic modulation of accuracy. (A) Estimated amplitude of the phasic modulation of subjects' and neural classifier's accuracy over time. Shaded areas around the curve denote between-subjects standard deviations, and dots at the bottom denote statistical significance, of which the lighter ones correspond to $p < 0.05$ uncorrected, and the darker ones correspond to those corrected (FDR = 0.05) for multiple comparisons. **(B)** Estimated amplitude of the phasic modulation of subjects' and neural classifier's accuracy at the time point 100 ms before stimulus onset in the functionally-defined ROIs. Thinner lines denote data from individual subjects, with the gray ones denoting cases where the estimated amplitude failed to exceed that of the null distribution. Thick black lines denote the mean amplitudes over all subjects. **(C)** Parcels showing significant phasic modulation of accuracy and the corresponding time courses of estimated amplitude. Same conventions as in (A).